ACS OMEGA

Open Access

http://pubs.acs.org/journal/acsodf

Article

Phytogenic-Mediated Zinc Oxide Nanoparticles Using the Seed Extract of *Citrullus lanatus* and Its Integrated Potency against Multidrug Resistant Bacteria

Munaza Hayat, Abdul Rehman,* Faheem Ahmed Khan, Muhammad Anees, Iffat Naz, Muhammad Qasim, and Nosheen Kanwal*

Cite This: *ACS Omega* 2024, 9, 16832−16841

Read Online

ACCESS | Metrics & More | Article Recommendations

ABSTRACT: In the current research study, zinc oxide nanoparticles (ZnO-NPs) were synthesized via a green synthesis technique using the seed extract of *Citrullus lanatus*. The study further intended to evaluate the potential synergistic effects of ZnO-NPs with antibiotics against multidrug resistant (MDR) bacteria. It was observed that *C. lanatus* seed extracts obtained by *n*-hexane and methanolic solvents revealed the presence of constituents, such as tannins, flavonoids, and terpenoids. Furthermore, the extract of *n*-hexane displayed the strongest antibacterial activity against *Yersinia* species (17 ± 1.2 mm) and *Escherichia coli* (17 ± 2.6 mm), while the methanolic extract showed the maximum antibacterial activity against *E. coli* (17 ± 0.8 mm). Additionally, the ZnO-NP synthesis was confirmed by ultraviolet-visible analysis with a characteristic absorption peak at 280 nm. The Fourier transform infrared spectroscopy analysis suggested the absorption peaks in the 500−3800 cm^{-1} range, which corresponds to various groups of tertiary alcohol, aldehyde, amine, ester, aromatic compounds, thiol, amine salt, and primary amine. The scanning electron microscopy spectra of ZnO-NPs demonstrated the presence of zero-dimensional spherical particles with well-dispersed character. Moreover, encapsulation with ZnO-NPs improved the antimicrobial activity of antibiotics against the panel of MDR bacteria, and the increases in the effectiveness of particular antibiotics against MDR bacteria were significant ($P = 0.0005$). In essence, the synthesized ZnO-NPs have the potential as drug carriers with powerful bactericidal properties that work against MDR bacterial strains. These outcomes are an indication of such significance in pharmaceutical science, giving possibilities for further research and development in this field.

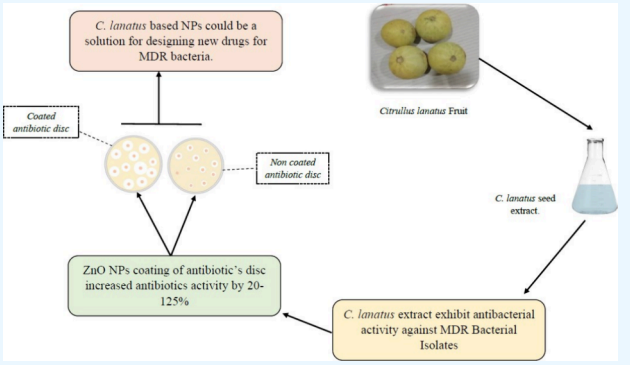

1. INTRODUCTION

In medical practice, antibiotics are the main therapeutic agents used for the treatment of bacterial infections.[1] Nevertheless, the problem of bacterial resistance is a complex situation, with a high rate of development of resistance mechanisms by bacteria, such as diminished drug penetration, modification of an antibiotic's target sites, inactivation of the drug, and efflux pump.[2,3] The World Health Organization (WHO) stresses the severity of the situation by citing MDR bacterial infections as a huge, alarming threat for global morbidity and mortality.[4] Annual deaths from MDR bacterial infections surpass the sum of those from cancer and diabetes, which underscores the need for alternative practices. In 2015, the WHO announced the approval of the Global Action Plan on Antimicrobial Resistance cementing the urgency for new approaches toward fighting this resistance phenomenon.[5−7]

Currently, studies are being conducted to look for new antimicrobial compounds, with the main focus on those based on metal chemistry.[8] The fact that silver, aluminum, copper, and zinc have been employed historically as microbicidal agents is backed by antiquity.[9,10] Among all metal nanoparticles, zinc in zinc oxide nanoparticle form has gained lots of interest for its strong antibacterial capacity at low quantities and effectiveness against different types of bacteria.[11] ZnO-NPs substantially demonstrate antimicrobial properties; therefore, they are important for applications of antibacterials.[12,13] Whether exposed to ultraviolet rays or not, their ability to produce reactive oxygen species enables them to kill bacteria even more effectively. Furthermore, in nanomedicine research, ZnO-NPs are becoming increasingly important constituents

Received: February 18, 2024
Revised: March 8, 2024
Accepted: March 12, 2024
Published: March 28, 2024

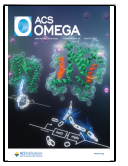

because they show low toxicity to mammalian cells, which gives them the possible option to be used as biomedical products.[14−16]

Different synthesis techniques, such as chemical, physical, and green methodologies, are employed to synthesize ZnO-NPs. The practice of chemical methods, which brings inherent environmental problems in the form of toxic chemicals, limits the application in the field of biocompatibility.[17] Physical techniques, like mechanical milling, allow us to manage the size of particles, but it has a side effect of contamination and high energy requirement.[18] Contrary to this, the green synthesis approach that utilizes plant extracts and microorganisms is getting more and more popular because it is environmentally safe. Green synthesis not only eliminates the risk of toxic chemical use but also operates at mild temperatures for less energy consumption.[19] Furthermore, the green method of ZnO-NP synthesis provides them a biocompatibility feature, thus making them a suitable alternative for biomedical applications as opposed to chemically and physically synthesized nanoparticles.[20,21] Consequently, chemical and physical methods might have some benefits, but green synthesis turns out to be a better substitute for the synthesis of ZnO-NPs.

Watermelon (*Citrullus lanatus*), originating from tropical Africa, is a substantial fruit characterized by its large oblong, ovoid, or roundish shape, featuring a hard green or white rind that is often variegated or striped.[22] The sweet, watery pulp of *C. lanatus* comes in pink, yellowish, or red hues and contains numerous seeds. Notably, *C. lanatus* derives its name from its high-water content, constituting about 68% pulp, 30% rind, and 2% seeds, possessing a nutritious profile, and offering a thirst-quenching, low-calorie option. Scientific interest in *C. lanatus* has flourished in recent years, focusing on its bioactivities.[23] The seeds of *C. lanatus* serve as a natural reservoir of various phytochemicals, including phenols, saponins, tannins, flavonoids, and alkaloids.[24−26] Remarkably rich in protein, tannins, minerals, citrulline (a precursor of L-arginine), beta-carotene, vitamin C, and lycopene,[27,28] these seeds have garnered attention for their nutritional composition and potential health benefits.

The therapeutic and pharmacological significance of *C. lanatus* are rooted in its unique composition. Phytochemical compounds in watermelon seeds, such as cucurbitacins and their glycoside derivatives, exhibit potent biological activities, including hepatoprotective, anti-inflammatory, antitumor, antimicrobial, and anthelmintic effects.[19,29−31] Traditional medicinal uses of *C. lanatus* are observed in Sudan for treating gastrointestinal disorders, rheumatism, inflammation, and gout, while in South Africa, its leaves and fruits are utilized in alternative medicinal therapies to address hypertension. Roasted *C. lanatus* seeds are employed as appetite stimulants and for alleviating constipation.[32−34]

The current study addresses a critical research gap by introducing a novel green synthesis method for ZnO-NPs using *C. lanatus* seed extract. The primary purpose is to develop an eco-friendly and biocompatible alternative to chemical and physical synthesis methods, highlighting the unique phytochemical composition of *C. lanatus* seeds. The study mainly focused on combating antibiotic resistance by evaluating the antibacterial potency of synthesized ZnO-NPs, particularly against MDR bacteria. The significance of the research lies in its potential to provide a sustainable solution to the global health crisis of antibiotic resistance, offering a biocompatible nanoparticle option for medical applications. Additionally, the study explores the therapeutic potential of *C. lanatus* seeds, contributing to a broader understanding of their bioactivities and medicinal applications.

2. MATERIALS AND METHODS

2.1. Collection of MDR Bacteria. The study comprised eight MDR bacterial isolates collected from the Microbiology Research Laboratory, Abasyn University Peshawar, Pakistan. The bacterial isolates included *Pseudomonas* spp., *Klebsiella* spp., Methicillin-resistant *Staphylococcus aureus*, *E. coli*, *Proteus* spp., *Yersinia* spp., *Providencia* spp., and *Morganella* spp. The isolates were reinoculated in nutrient agar media and verified through conventional culturing techniques. The MDR bacteria were cultured in nutrient broth, and they were stored in glycerol (15% at −80 °C) for further analysis.

2.2. Collection and Processing of *C. lanatus* Fruit. The fruit samples of *C. lanatus* were collected aseptically in sterile polyethylene bags from different areas of District Mianwali, Punjab, Pakistan. After collection, the outermost skin covering of *C. lanatus* fruit was removed with a peeler, and then, the seeds were extracted. The seeds were rinsed with tap water, spread on newspapers, and left to dry for almost 2 weeks at room temperature. The dried seeds were then grounded into a powder form using an electrical grinder (model: FOSS cyclotec 1093, Sweden). The powdered seed material was collected in an airtight jar with a screw cap and stored at room temperature (25 °C).

2.3. Preparation of *n*-Hexane and Methanolic Extracts. Approximately 25 g of finely powdered seed extract was separately soaked in two different flasks: one containing 150 mL of *n*-hexane and the other containing 150 mL of a methanolic solution. The solutions were vigorously mixed and left to stand at 25 °C overnight. Given the high volatility of *n*-hexane, the rotary evaporation process was conducted for an optimized period of 4 h at 150 rpm, ensuring efficient extraction of lipophilic compounds. The resulting crude extracts were then prepared into final activity solutions using dimethyl sulfoxide (DMSO) as a solvent before undergoing further analysis.[35]

2.5. Phytochemical Analysis of Seed Extracts of *C. lanatus*. The phytochemical analyses of the *n*-hexane and methanolic seed extracts of *C. lanatus* were carried out, and the presence of different phytoconstituents, including flavonoids, saponins, tannins, terpenoids, and phenolic compounds, was reported using qualitative chemical tests.[36]

2.6. Antibacterial Activity of Seed Extracts of *C. lanatus*. The antibacterial activity of *C. lanatus* seed extracts against the tested MDR bacterial isolates was evaluated by using the agar well diffusion method. A suspension of each MDR isolate was prepared by suspending a full loop in 1 mL of normal saline, and subsequently, 50 μL of the suspension was inoculated onto Mueller Hinton agar (MHA) media. Four wells (6 mm diameter) were bored in each plate using a sterile cork borer. One well was used for the negative control (1% DMSO), one well was used for the positive control (antibiotics), and the remaining two wells were used for extracts of *C. lanatus*. The culture plates were incubated at 37 °C for 24 h, and the inhibition zones were measured according to CLSI guidelines as prescribed by PA.[37]

2.7. Synthesis of ZnO-NPs. For the synthesis of ZnO-NPs, 10 g of *C. lanatus* seed powder was added into a 400 mL distilled water glass bottle. Subsequently, the mixture was

https://doi.org/10.1021/acsomega.4c01554
ACS Omega 2024, 9, 16832−16841

heated for 5−6 min in a water bath set at 60 °C. Following this, the mixture was transferred to a rotary shaker and incubated at 37 °C while rotating at 150 rpm for 24 h. The change of color from an orange to a yellowish precipitate indicated the formation of $Zn(OH)_2$ powder. The mixture was then filtered through Whatman No. 1 filter paper and was further used for the synthesis of ZnO-NPs.[35]

In a glass reagent bottle, approximately 30 mL of the *C. lanatus* filtrate was mixed with 30 mL of 1 mM $ZnSO_4{\cdot}7H_2O$ and gently shaken until a solution was formed. The pH was brought to 12 by adding 1 mM NaOH, after which the mixture was subjected to centrifugation at 3000 rpm for 5 min. The cells at the bottom of the tube were harvested, cleaned with 70% ethanol, and then placed in a Petri dish. The precipitate, which was therefore obtained as a dried form, was kept in a glass container at 4 °C and covered with aluminum foil to shield it from the daylight.[35]

2.8. Characterization of ZnO-NPs. Characterization of ZnO-NPs was accomplished with state-of-the-art techniques including UV-visible spectroscopy, SEM, X-ray diffraction (XRD), energy-dispersive analysis of X-rays (EDAX), and FTIR at the Pakistan Council of Scientific Research. The UV−vis spectrophotometric analysis was performed using a machine (UV-1901 Agilent Technology, Cary series UV−vis spectrometer, USA) to scan the wavelength range of 200−800 nm with a scan speed of 480 nm/min to obtain the absorption spectra of ZnO-NPs. SEM (Philips SEM, CMC-300 kV model, Netherland) was used for high-resolution micrographs of synthesized ZnO-NPs at magnifications of 1000× and 10,000× obtaining a voltage of 160 kV. Further to this, the elemental composition of zinc and oxygen was expressed using EDX, which was used together with SEM. Additionally, FTIR was performed using a PerkinElmer FTIR spectrometer (GX Model, USA) to examine distinct peaks and analyze different functional groups by the KBr pellet method. To determine the patterns (crystalline or amorphous nature) of synthesized nanoparticles, XRD measurement was carried out using a diffractometer (Ultima IV, Rigaku, Japan) set at 40 kV and 30 mA at a specific scanning rate (20 min^{-1}), from 25 to 800, using a nickel-filtered Cu at room temperature with λ = 1.542 Å.

2.9. Preparation of Antibiotic Discs Coated with ZnO-NPs. The ZnO-NPs were coated on different antibiotic discs (nitrofurantoin (100 μg), cefepime (30 μg), ceftazidime (30 μg), amoxicillin (25 μg), imipenem (10 μg), ciprofloxacin (6 μg), and piperacillin + tazobactam (11 μg)). For this purpose, ZnO-NP powder (20 mg) was dissolved in sterile distilled water (1 mL) to prepare a nanopowder suspension with a final concentration of 20 μg/μL. Next, under sterile conditions, the selected antibiotic discs were taken in a dry Petri plate. Using a pipet, 5 μL of suspension, containing 100 μg of ZnO-NPs, was applied to each antibiotic disc to coat them. The coated discs were then dried completely in an oven for at least 15 min at 60 °C.

2.10. *In Vitro* Assay. Both the coated and noncoated antibiotic discs were tested using Kirby Bauer's disc diffusion method against the selected MDR bacteria on Muller−Hinton agar plates. The discs were located with sterile forceps and pressed gently to allow contact with the bacterial lawn, and then, plates were incubated for 24 h at 37 °C. The inhibition zone's "diameter" was measured according to the Clinical and Laboratory Standards Institute's guidelines.[37]

2.11. Statistical Analysis. The experiments were performed in triplicate, and the Microsoft Excel 2013 program was employed to calculate mean values of zones of inhibition of antibiotics against MDR bacteria. A *t* test was conducted to determine the statistical significance with a *P*-value of less than 0.05.

3. RESULTS

3.1. Phytochemical Analysis of *C. lanatus* Seed Extracts. The *n*-hexane and methanolic extracts of *C. lanatus* seeds were examined for phytochemical analysis. It was observed that both extracts of *C. lanatus* contained different phytoconstituents such as tannins, flavonoids, and terpenoids, while phenolic compounds and saponins were absent in both extracts (see Table 1).

Table 1. Phytochemical Analysis of *C. lanatus* Seed Extracts[a]

components	*n*-hexane extract	methanolic extract
phenolic compounds	-	-
saponins	-	-
tannin	+	++
flavonoid	++	+++
terpenoids	+++	+

[a]-, absent; +, little bit color; ++, intermediate; +++, strong.

3.2. Antibacterial Activity of *n*-Hexane and Methanolic Extracts of *C. lanatus*. In the current study, two different concentrations (50 and 100 μL) were used to evaluate the antibacterial activity of *n*-hexane and methanolic extracts against tested MDR bacteria. It was observed that at both concentrations, *n*-hexane extracts displayed antibacterial activity against the tested MDR bacterial isolates; however, at a concentration of 50 μL, it displayed the highest antibacterial activities of 14 ± 2.6 mm against *E. coli* while, at a concentration of 100 μL, showing the maximum antibacterial activities of 17 ± 1.2 mm against *Yersinia* spp., as shown in Figure 1.

Similarly, at a 50 μL concentration, the highest antibacterial activity of methanolic extract was observed against *E. coli* (17 ± 0.8 mm) followed by *Pseudomonas* spp. (13 ± 0.8 mm), *Yersinia* spp. (12 ± 0.5 mm), *Klebsiella* spp. (11 ± 1.2 mm), *Providencia* spp. (11 ± 1.2 mm), MRSA (10 ± 1.2 mm), *Proteus* spp. (9 ± 0.5 mm), and *Morganella* spp. (9 ± 0.9 mm). Meanwhile, at a 100 μL concentration, strong activity was observed against *E. coli* (18 ± 0.5 mm) followed by *Pseudomonas* spp. (17 ± 1.5 mm), MRSA (15 ± 2.5 mm), *Yersinia* spp. (15 ± 1.0 mm), *Klebsiella* spp. (15 ± 1.5 mm), *Providencia* spp. (14 ± 0.6 mm), *Morganella* spp. (13 ± 1,5 mm), and *Proteus* spp. (12 ± 1.5 mm), as shown in Figure 2.

3.3. Characterization of ZnO-NPs. The UV−vis spectrum of the synthesized ZnO-NPs was observed (Figure 3). The λ max for the sample was 280 nm, giving the characteristic peak of the ZnO-NPs.

In the current study, the SEM micrographs of the synthesized ZnO-NPs showed dispersed, spherical particles with zero dimension. The average sizes were about 10 μm at a magnification of 1000× (image a) and 1 μm at a magnification of 10,000× (image b), which was determined using Image-J software (Figure 4).

The required elements, including zinc (Zn) and oxygen (O), as revealed by the EDAX spectrum, were present in the sample

https://doi.org/10.1021/acsomega.4c01554
ACS Omega 2024, 9, 16832−16841

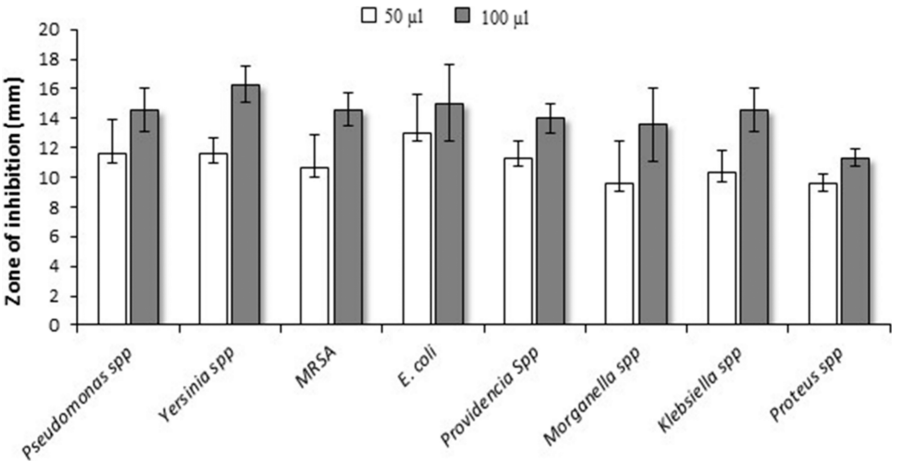

Figure 1. Antibacterial activity of *n*-hexane extracts of *C. lanatus* seeds against tested MDR bacterial isolates (P = 0.0002).

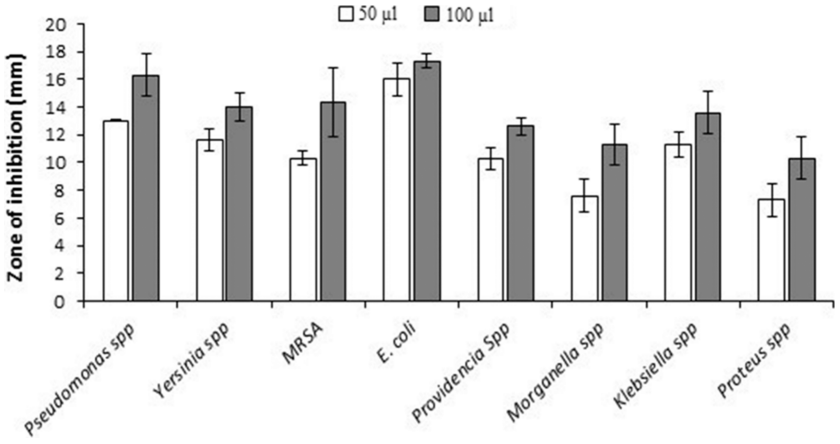

Figure 2. Antibacterial activity of methanolic extracts of *C. lanatus* seeds against tested MDR bacterial isolates (P = 0.0497).

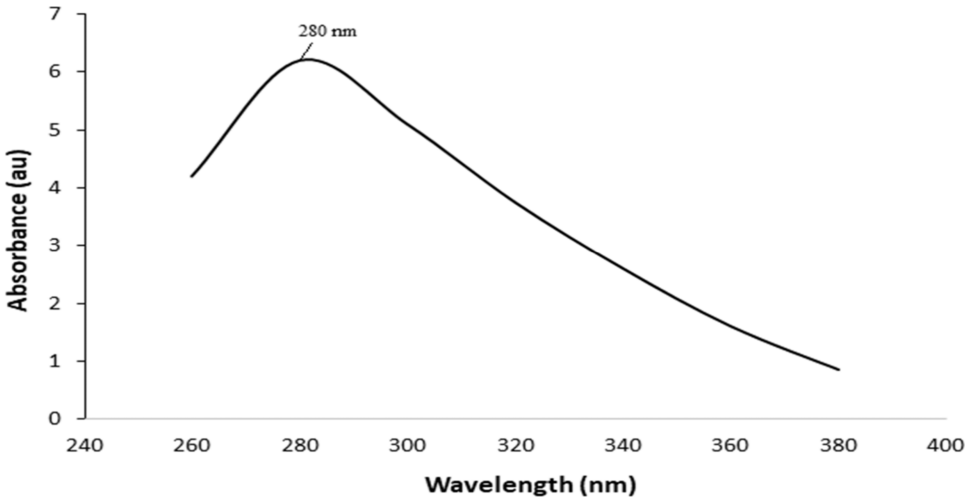

Figure 3. UV−vis spectrum of synthesized ZnO-NPs (absorption peak value at 280 nm).

and confirmed the purity of the ZnO-NPs. The presence of other elements, including phosphorus (P), magnesium (Mg), potassium (K), and sulfur (S), was also observed in small amounts (Figure 5).

FTIR analysis was used to estimate the purity and nature of ZnO-NPs as well as to identify the presence of different functional groups. In the current study, the FTIR spectrum contains a range of absorption peaks between 500 and 3800 cm^{-1}, indicative of different functional groups. These peaks included alkene (C−H) at 917 cm^{-1}, tertiary alcohol (C−O) at 1180 cm^{-1}, aldehyde (C−H) at 1380 cm^{-1}, amine (N−H) at 1628 cm^{-1}, ester (C═O) at 1731 cm^{-1}, aromatic compounds (C−H bending) at 1982 cm^{-1}, CO_2 (O═C═O) at 2372 cm^{-1}, thiol (S−H stretching) at 2630 cm^{-1}, amine

https://doi.org/10.1021/acsomega.4c01554
ACS Omega 2024, 9, 16832−16841

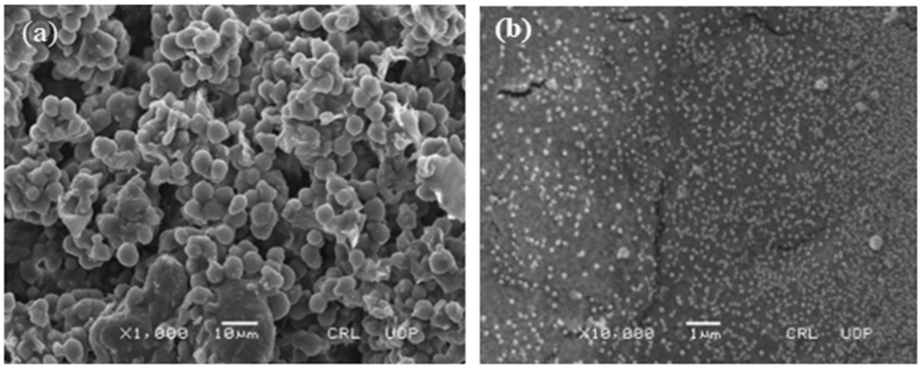

Figure 4. SEM micrograph of synthesized ZnO-NPs. The average size of seed synthesized ZnO-NPs (a) at a magnification of 1000×, while (b) at a magnification of 10,000×.

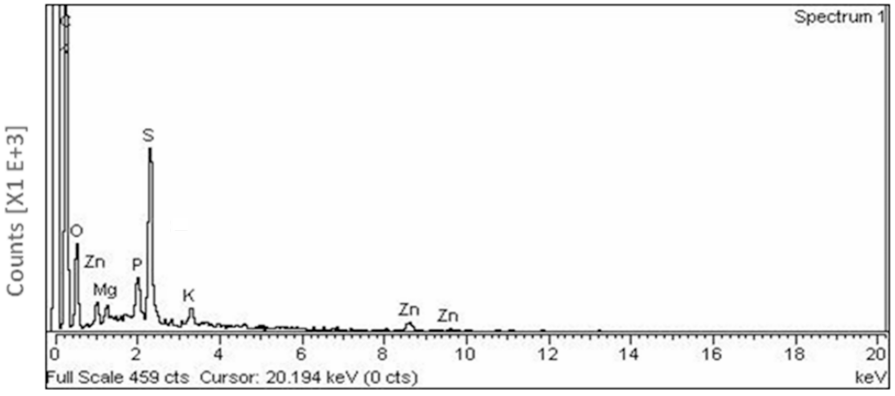

Figure 5. EDAX spectra of synthesized ZnO-NPs.

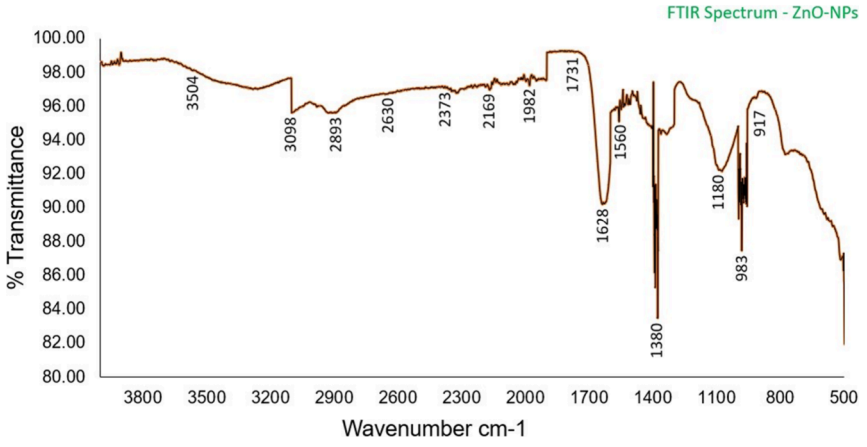

Figure 6. FTIR spectra of synthesized ZnO-NPs.

salt (N−H) at 2893 cm^{-1}, alkene (C−H) at 3098 cm^{-1}, and primary amines (N−H) at 3504 cm^{-1} (Figure 6).

The phase purity and composition of the synthesized ZnO-NPs were evaluated by an XRD analysis. The XRD measurement results indicated an average size of 40 nm with a crystalline structure of ZnO-NPs. The sharp peak shows the Bragg reflection indexed at $2\theta = 28.9°$, as illustrated in Figure 7.

3.4. Antibacterial Activity of ZnO-NP-Coated and Noncoated Antibiotics. The effectiveness of ZnO-NP-coated and noncoated antibiotics against MDR bacteria was assessed using a standard technique. The results demonstrated an enhancement in the antibiotic's efficacy upon coating with ZnO-NPs. In the case of ZnO-NP-coated nitrofuran, a maximum potency of 20.5% was observed against *Klebsiella* spp., ceftazidime up to 58.2% against *Morganella* spp., imipenem up to 57.2% against *Klebsiella* spp., and amoxicillin up to 28.7% against *Morganella* spp. Similarly, ciprofloxacin showed a maximum potency of 125% against *Providencia* spp. followed by cefepime (31.7%) against *Providencia* spp., while piperacillin + tazobactam showed a potency of 25.8% against *E. coli* (Table 2).

4. DISCUSSION

This study was conducted with the primary objective of synthesizing ZnO-NPs through the utilization of *C. lanatus*

https://doi.org/10.1021/acsomega.4c01554
ACS Omega 2024, 9, 16832−16841

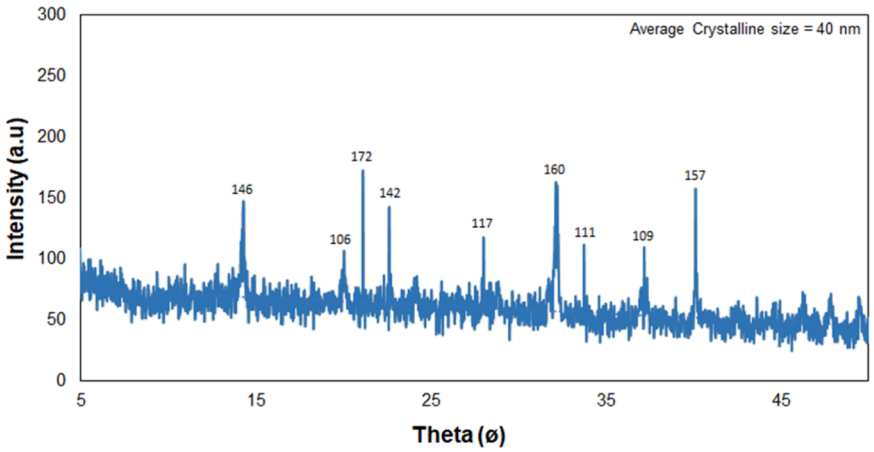

Figure 7. XRD spectrum of synthesized ZnO-NPs (the Bragg reflection indexed at $2\theta = 28.9^{\circ}$ with an average particle size of 40 nm).

Table 2. Activity of ZnO-NP Coated and Noncoated Antibiotics against Test MDR Isolates[a]

		activity of ZnO-NP-coated and noncoated antibiotics against MDR bacteria (mm)								
antibiotics used in activity		*MRSA*	*E. coli*	*Pseudomonas* spp.	*Morganella* spp.	*Proteus* spp.	*Providencia* spp.	*Klebsiella* spp.	*Yersinia* spp.	*P*-value
nitrofuran	uncoated	14 ± 0.2	15.5 ± 0.4	14.6 ± 0.1	14 ± 0.2	14.6 ± 0.3	13.6 ± 0.2	14.6 ± 0.1	14 ± 0.3	0.0105
	ZnO-NP-coated	14.5 ± 0.3	16.6 ± 0.7	16 ± 0.4	15.6 ± 0.2	15.3 ± 0.5	15.3 ± 0.4	17.6 ± 0.3	14.3 ± 0.5	
	potency %	3.57%	7.09%	9.58%	11.43%	11.43%	12.5%	20.55%	2.14%	
ceftazidime	uncoated	13.6 ± 0.3	12.3 ± 0.3	11.6 ± 0.3	10.3 ± 0.3	12.3 ± 0.3	8 ± 0.2	12.6 ± 0.2	13.6 ± 0.3	0.0005
	ZnO-NP-coated	16.3 ± 0.2	15.3 ± 0.2	15.6 ± 0.4	16.3 ± 0.2	15.3 ± 0.2	12.6 ± 0.3	17.6 ± 0.6	15.2 ± 0.4	
	potency %	19.85%	24.4%	34.5%	58.3%	24.4%	57.5%	39.7%	11.8%	
imipenem	uncoated	9.6 ± 0.1	10.6 ± 0.5	10 ± 0.2	10.3 ± 0.1	10.3 ± 0.1	10.6 ± 0.6	11 ± 0.7	9.6 ± 0.1	0.0023
	ZnO-NP-coated	13.6 ± 0.3	16 ± 0.3	14 ± 0.4	15 ± 0.3	16 ± 0.4	15.3 ± 0.4	17.3 ± 0.5	14.3 ± 0.6	
	potency %	41.66%	50.9%	40%	45.63%	55.3%	44.3%	57.3%	48.95%	
amoxicillin	uncoated	9.6 ± 0.5	8 ± 0.4	9 ± 0.3	8 ± 0.2	8.6 ± 0.5	10 ± 0.3	10.5 ± 0.1	8.3 ± 0.3	0.0112
	ZnO-NP-coated	10 ± 0.4	9.6 ± 0.4	9.6 ± 0.4	10.3 ± 0.5	10.2 ± 0.2	10.6 ± 0.5	11 ± 0.3	9.6 ± 0.5	
	potency %	4.1%	20%	6.67%	28.6%	18.6%	6%	4.8%	15.6%	
ciprofloxacin	uncoated	9 ± 0.3	8 ± 0.3	8.6 ± 0.3	8 ± 0.3	8 ± 0.7	8 ± 0.1	8.6 ± 0.3	8.3 ± 0.3	0.0031
	ZnO-NP-coated	14 ± 0.4	14.3 ± 0.2	14 ± 0.5	15.6 ± 0.4	16 ± 0.4	18 ± 0.3	15.3 ± 0.5	14.3 ± 0.2	
	potency %	55.5%	78.8%	63%	95%	99.8%	125%	78%	72.3%	
cefepime	uncoated	14.6 ± 0.2	16 ± 0.3	17.6 ± 0.3	14.3 ± 0.2	15.3 ± 0.2	13.2 ± 0.8	11 ± 0.7	15.6 ± 0.3	0.0034
	ZnO-NP-coated	19 ± 0.5	18.3 ± 0.5	19.6 ± 0.4	18.6 ± 0.7	19.3 ± 0.5	17.4 ± 0.6	13.6 ± 0.3	20.3 ± 0.2	
	potency %	30.2%	14.4%	11.4%	30.07%	26.2%	31.7%	23.7%	30.13%	
piperacillin + tazobactam	uncoated	15.3 ± 0.2	14.3 ± 0.2	17 ± 0.2	16 ± 0.1	15 ± 0.2	14.6 ± 0.3	15 ± 0.3	14 ± 0.3	0.0002
	ZnO-NP-coated	18.3 ± 0.3	18 ± 0.4	19 ± 0.5	16.6 ± 0.3	17.3 ± 0.1	16 ± 0.5	18 ± 0.5	17.3 ± 0.1	
	potency %	19.6%	25.87%	11.76%	3.75%	15.33%	9.6%	20%	23.6%	

[a]ZnO-NPs, zinc oxide nanoparticles; %, percentage; spp., species.

seed extract. The synthesized ZnO-NPs were assessed for their ability to augment the efficacy of antibiotics against MDR bacteria, which include *Pseudomonas* spp., *Klebsiella* spp., Methicillin-resistant *S. aureus*, *E. coli*, *Proteus* spp., *Yersinia* spp., *Providencia* spp., and *Morganella* spp. Employing green synthesis technology, known for its eco-friendly, cost-effective, and efficient attributes, added a dimension of environmental sustainability to this research.[38,39] It is essential to note that ZnO-NPs have emerged as promising drug delivery carriers in modern scientific applications.[40]

The *n*-hexane and methanolic extracts of *C. lanatus* were subjected to a comprehensive phytochemical analysis. This analysis unveiled the presence of three key phytochemical groups: tannins, flavonoids, and terpenoids within both extracts, while phenolic compounds and saponins were notably absent (Table 1). These trials showed that the research

https://doi.org/10.1021/acsomega.4c01554
ACS Omega 2024, 9, 16832−16841

identifies the exact markers that in previous studies were linked to *C. lanatus* extracts.[29,41,42] On the other hand, both *n*-hexane and methanolic extracts were proven to have antibacterial activity against *E. coli* and *Yersinia* spp., highlighting the antibacterial property of their phytochemical components.[43]

Various types of analytical techniques were employed to gain a deeper understanding of the structural and optical properties of the synthesized ZnO-NPs. UV-visible spectroscopy showed a peak of 280 nm in its absorption, which has been reported as the surface plasmon resonance band of ZnO-NPs (Figure 3). These results agree with the finding of Husain et al.,[44] who reported a characteristic peak at 281 nm attributed to ZnO-NPs synthesized from *Plumbago zeylanica* extract. In the same way, the absorbance peaks of 284 and 345 nm were observed for ZnO-NPs of the leaf and flower extracts of pomegranate, respectively.

SEM scanning showed a convincing visual of the ZnO-NPs in which they were evenly distributed and had an irregular spherical shape. The nanoparticles responded with a size of 10 μm at the scale of the 1000× magnification and 1 μm at the scale of the 10,000× magnification (Figure 4). This implies that *C. lanatus* seed extract's antioxidants and other compounds are essential for efficiently lowering the production of unevenly shaped ZnO-NPs. This result aligned with the findings of Ifeanyichukwu et al.,[45] Umar et al.,[46] and Muhammad et al.[47] whose SEM micrographs of ZnO-NPs were irregular, though they had a spherical morphology and appeared to be agglomerated.

EDAX showed that the synthesized ZnO-NPs had a high purity, and there was a clear Zn peak at 20.194 kV and a clear O peak at the same energy. Moreover, small height peaks corresponding to magnesium (Mg), phosphorus (P), sulfur (S), and potassium (K) were observed indicating the biogenic production of the nanoparticles (Figure 5). Akhter et al.[48] also reported similar results of EDX analysis of ZnO-NPs produced from the leaf extract of *Swertia chirayita* that support the high purity of synthesized ZnO-NPs.

The FTIR spectrum of synthesized ZnO-NPs demonstrated peaks that were characteristic of different functional groups, giving a proper picture of the chemistry and properties of the nanoparticles. The recorded peak at 917 cm^{-1} of the (C−H) alkene group signifies the presence of organic compounds on the surface of ZnO-NPs. This result is consistent with the green synthesis technique that involves the use of plant extracts or other biologically derived materials. The presence of tertiary alcohol (C−O) at 1180 cm^{-1} indicated the presence of alcohol groups, possibly the reducing or stabilizing products in the green synthesis process. The carbonyl compound involved in the synthesis of nanoparticles was confirmed from the C−H peak of the aldehyde at 1380 cm^{-1}. Amine groups (N−H), a common case seen in biomediated synthesis, which were found at 1628 cm^{-1}, likely connected with the stabilizing or reducing agents. The peak marked (C═O) at 1731 cm^{-1} was attributed to the carbonyl groups from the organic capping agents that were used in the nanoparticle stabilization. Aromatic compounds (C−H bending) at 1982 cm^{-1} further suggested the contribution of aromatic components, potentially from the plant extract or other organic precursors used in the green synthesis. The CO_2 peak (O═C═O) at 2372 cm^{-1} could be attributed to environmental contamination or adsorption on the nanoparticle surface. The thiol (S−H stretching) peak at 2630 cm^{-1} indicated the presence of sulfur-containing compounds, likely originating from biological reducing agents. The amine salt peak at 2893 cm^{-1} suggested the involvement of organic salts in stabilizing the nanoparticles. Another alkene (C−H) peak at 3098 cm^{-1} underlined the presence of additional organic compounds, while the primary amine (N−H) peak at 3504 cm^{-1} further supported the association with bioreducing or stabilizing agents.

These observations strongly indicated the integration of different organic compounds originating from the *C. lanatus* seed extract within the fabricated nanoparticles. This alignment with the study conducted by El-Belely et al.[49] on *Arthrospira platensis* mediated ZnO-NP synthesis and displayed the inherent variability in organic substances across different plant sources. The consistent identification of specific functional groups, in both our experimental results and the literature, reinforces the reliability and reproducibility of ZnO-NPs. Furthermore, the efficacy of *C. lanatus* extract in the synthesis process not only facilitates the reduction, capping, and stabilization of ZnO-NPs but also imparts unique organic components to the final product. In corroboration, Chaudhuri and Malodia[50] conducted a similar study on ZnO-NPs synthesized from the leaf extract of *Calotropis gigantea*, noting analogous peaks indicative of characteristic OH and C−H stretching vibrations. Additionally, Azizi et al.[51] proposed that the formation of ZnO-NPs results from the interaction between oxygen as functional groups present in the plant extract and zinc molecules in salt precursors.

XRD analysis was employed to investigate the crystal structure of the ZnO nanoparticles, revealing a peak at 2θ = 29° corresponding to a Bragg reflection. This peak signifies the crystalline nature of the particles, and the average particle size was estimated to be 40 nm (Figure 7). These findings are in line with the work of Husain et al.,[44] who also identified a prominent peak at 35.56°, indicating the crystalline nature of ZnO-NPs with an average particle size of 43 nm.

The investigation into the enhanced antibacterial activity of antibiotics coated with ZnO-NPs against MDR bacteria is a pivotal aspect of this study. The observed interactions between ZnO-NPs and the bacterial cell wall play a central role in strengthening the antibiotic efficacy. The mechanisms involved include cell rupture, the generation of oxidative stress, and genotoxicity, collectively resulting in significant bacterial damage.[52,53]

The functional groups identified in synthesized ZnO-NPs, including alkene, tertiary alcohol, aldehyde, amine, ester, aromatic compounds, thiol, amine salt, alkene, and primary amines, collectively contribute to the complexed antibacterial effects observed in the coated antibiotics. One of the key mechanisms involves the generation of reactive oxygen species (ROS), which is supported by the presence of alkene groups known to participate in redox reactions (alkene at 917 cm^{-1}). The observed tertiary alcohol (C−O) and aldehyde (C−H) groups may further contribute to oxidative stress, disrupting bacterial membranes and enhancing the overall antibacterial activity.

The enhanced potency of ZnO-NP-coated antibiotics against tested MDR bacteria demonstrates a nuanced response to different antibiotic-bacterium interactions. For instance, the maximum potency was observed with nitrofuran against *Klebsiella* spp. (20.5%), ceftazidime against *Morganella* spp. (58.2%), imipenem against *Klebsiella* spp. (57.2%), amoxicillin against *Morganella* spp. (28.7%), ciprofloxacin against *Providencia* spp. (125%), cefepime against *Providencia* spp. (31.7%),

https://doi.org/10.1021/acsomega.4c01554
ACS Omega 2024, 9, 16832−16841

and piperacillin + tazobactam against *E. coli* (25.8%), as shown in Table 2.

The specific impact of ZnO-NPs on these antibiotics can be linked to their unique surface chemistry derived from the identified functional groups. The aromatic compounds, ester, and thiol groups, among others, contribute to the stability and reactivity of the nanoparticles, influencing antibiotic-bacterial interactions. Moreover, the generation of ROS, as a consequence of these functional groups, aligns with the well-established antimicrobial mechanisms of metal or metal oxide nanoparticles, as highlighted by Alavi and Yarani[54] in their studies. These results align with the findings of Akbar et al.,[55] who reported robust antibacterial effects of ZnO-NPs against *Salmonella typhimurium* and *S. aureus*.[56−58] Moreover, other studies have demonstrated the potent bactericidal and antifungal activities of ZnO-NPs against a spectrum of pathogens.[59,60]

5. CONCLUSIONS

It was concluded that the seed extract of *C. lanatus* was an excellent source and had a maximum capacity to synthesize ZnO-NPs at room temperature. Moreover, the UV−vis spectrum of synthesized ZnO-NPs indicated an absorption peak at 280 nm within the prescribed range, while the SEM micrograph demonstrated the dispersed, spherical morphology of ZnO-NPs, the EDAX spectrum indicated the extent of zinc (Zn), phosphorus (P), magnesium (Mg), sulfur (S), and potassium (K) in ZnO-NPs. Similarly, FTIR analysis confirmed the presence of diverse functional groups, including alkene, ester, thiol, and amine, acting as effective capping and stabilizing agents on the ZnO-NP surface. These agents, originating from green synthesis and bioderived materials, contribute to the nanoparticles' stability and reactivity, ultimately enhancing antibiotic potency against MDR bacteria. On the other hand, the XRD peak confirmed the phase purity, size, internal crystalline structure, and nature of the synthesized ZnO-NPs. Furthermore, the antimicrobial efficacy of antibiotics against the MDR bacterial isolates was augmented by coating with ZnO-NPs. While the synthesis and antibacterial potential of ZnO-NPs from *C. lanatus* seeds are highlighted, it is essential to recognize study limitations. Further investigations into specific mechanisms, potential cytotoxic effects, and a thorough assessment of long-term stability and *in vivo* implications are warranted for comprehensive applicability in the pharmaceutical and medical domains.

AUTHOR INFORMATION

Corresponding Authors

Abdul Rehman − *Department of Microbiology, Kohat University of Science and Technology (KUST), Kohat, Khyber Pakhtunkhwa 26000, Pakistan;* orcid.org/0000-0001-9004-6384; Email: abdulrehman@kust.edu.pk

Nosheen Kanwal − *Department of Chemistry, College of Sciences, Qassim University, Buraidah 51452, Saudi Arabia*; Email: No.khan@qu.edu.sa

Authors

Munaza Hayat − *Department of Microbiology and Biotechnology, Faculty of Life Sciences, Abasyn University Peshawar Campus, Peshawar, Khyber Pakhtunkhwa 25000, Pakistan*

Faheem Ahmed Khan − *Department of Allied Health Sciences, Iqra National University, Peshawar, Khyber Pakhtunkhwa 25000, Pakistan*

Muhammad Anees − *Department of Microbiology, Kohat University of Science and Technology (KUST), Kohat, Khyber Pakhtunkhwa 26000, Pakistan*

Iffat Naz − *Department of Biology, College of Science, Qassim University, Buraydah 51452, Saudi Arabia*

Muhammad Qasim − *Department of Microbiology, Kohat University of Science and Technology (KUST), Kohat, Khyber Pakhtunkhwa 26000, Pakistan*

Complete contact information is available at: https://pubs.acs.org/10.1021/acsomega.4c01554

Author Contributions

Conceptualization, methodology, and supervision: A.R. and F.A.K.; data collection and processing: M.H.; formal analysis and writing-original draft manuscript: A.R., M.A., and I.N.; critical review and editing: N.K. and M.Q. All the authors have read and approved the final version of the manuscript.

Funding

Deanship of Scientific Research, Qassim University, Saudi Arabia.

Notes

The authors declare no competing financial interest.

The authors declare that they have no known competing financial interests or personal relationships that could have appeared to influence the work reported in this paper.

ACKNOWLEDGMENTS

Researchers would like to thank the Deanship of Scientific Research, Qassim University for funding the publication of this project.

REFERENCES

(1) Bisher, M. A.; Al Bisher, M. A.; Albeshr, H. D.; Alsagoor, N. A.; Alqureshah, H. M.; Al Hutaylah, M. M.; Al Komssan, M. S.; Almansour, M. S.; Alabbas, A. Y.; Al Yami, W. H.; Al Yami, R. H. Impact of Self-medications and Medications Misuse on Health Outcomes. *Anal. Clin. Anal. Med.* **2023**, *10* (1), 932−939.

(2) Hou, J.; Long, X.; Wang, X.; Li, L.; Mao, D.; Luo, Y.; Ren, H. Global trend of antimicrobial resistance in common bacterial pathogens in response to antibiotic consumption. *J. Hazard. Mater.* **2023**, *442*, No. 130042.

(3) El-Kattan, N.; Emam, A. N.; Mansour, A. S.; Ibrahim, M. A.; Abd El-Razik, A. B.; Allam, K. A.; Riad, N. Y.; Ibrahim, S. A. Curcumin assisted green synthesis of silver and zinc oxide nanostructures and their antibacterial activity against some clinical pathogenic multi-drug resistant bacteria. *RSC Adv.* **2022**, *12* (28), 18022−18038.

(4) World Health Organization. *Global action plan on antimicrobial resistance*. WHO: Geneva, Switzerland (2015). https://www.amcra.be/swfiles/files/WHO%20actieplan_90.pdf.

(5) Gold, K.; Slay, B.; Knackstedt, M.; Gaharwar, A. Antibacterial activity of metal and metal-oxide based nanoparticles. *Adv. Ther* **2018**, *1* (3), 1700033.

(6) Zaman, S. B.; Hussain, M. A.; Nye, R.; Mehta, V.; Mamun, K. T.; Hossain, N. A review on antibiotic resistance: alarm bells are ringing. *Cureus* **2017**, *9* (6), No. e1403.

(7) World Health Organization. *World Health Statistics 2014*. WHO: Geneva, Switzerland (2014). https://www.who.int/docs/default-source/gho-documents/world-health-statistic-reports/world-health-statistics-2014.pdf.

(8) Ali, G.; Khan, A.; Shahzad, A.; Alhodaib, A.; Qasim, M.; Naz, I.; Rehman, A. Phytogenic-mediated silver nanoparticles using *Persicaria*

hydropiper extracts and its catalytic activity against multidrug resistant bacteria. *Arab. J. Chem.* **2022**, *15* (9), No. 104053.
(9) Lemire, J. A.; Harrison, J. J.; Turner, R. J. Antimicrobial activity of metals: mechanisms, molecular targets and applications. *Nat. Rev. Microbiol.* **2013**, *11* (6), 371−384.
(10) Turner, R. Metal-based antimicrobial strategies. *Microb. Biotechnol.* **2017**, *10* (5), 1062−1065.
(11) Deshmukh, C. D.; Jain, A.; Tambe, M. S. Phytochemical and pharmacological profile of *Citrullus lanatus* (THUNB). *Biolife.* **2015**, *3* (2), 483−488.
(12) Yusof, H. M.; Mohamad, R.; Zaidan, U. H.; Samsudin, A. A. Optimization of biosynthesis zinc oxide nanoparticles: Desirability-function based response surface methodology, physicochemical characteristics, and its antioxidant properties. *OpenNano.* **2022**, *8*, No. 100106.
(13) Sánchez-López, E.; Gomes, D.; Esteruelas, G.; Bonilla, L.; Lopez-Machado, A. L.; Galindo, R.; Cano, A.; Espina, M.; Ettcheto, M.; Camins, A.; Silva, A. M. Metal-based nanoparticles as antimicrobial agents: an overview. *Nanomaterials.* **2020**, *10* (2), 292.
(14) Alhujaily, M.; Albukhaty, S.; Yusuf, M.; Mohammed, M. K.; Sulaiman, G. M.; Al-Karagoly, H.; Alyamani, A. A.; Albaqami, J.; AlMalki, F. A. Recent advances in plant-mediated zinc oxide nanoparticles with their significant biomedical properties. *Bioengineering.* **2022**, *9* (10), 541−559.
(15) Zhang, L.; Jiang, Y.; Ding, Y.; Povey, M.; York, D. Investigation into the antibacterial behaviour of suspensions of ZnO nanoparticles (ZnO nanofluids). *J. Nanopart. Res.* **2007**, *9* (3), 479−489.
(16) Rasmussen, J. W.; Martinez, E.; Louka, P.; Wingett, D. G. Zinc oxide nanoparticles for selective destruction of tumor cells and potential for drug delivery applications. *Expert. Opin. Drug. Delivery* **2010**, *7* (9), 1063−1077.
(17) Kumar, B.; Smita, K.; Cumbal, L.; Debut, A. Synthesis of ZnO nanoparticles using leaf extract of *Calotropis gigantea*: characterization and their evaluation as photocatalysts. *J. Photochem. Photobiol. B: Biol.* **2011**, *104* (1−2), 1−7.
(18) Huang, J.; Li, Q.; Sun, D.; Lu, Y.; Su, Y.; Yang, X.; Wang, H.; Wang, Y. Biosynthesis of silver and gold nanoparticles by novel sundried Cinnamomum camphora leaf. *Nanotechnology* **2007**, *18* (10), No. 105104.
(19) Alavi, M.; Hamblin, M. R.; Kennedy, J. F. Antimicrobial applications of lichens: secondary metabolites and green synthesis of silver nanoparticles: a review. *Nano. Micro. Biosystems.* **2022**, *1* (1), 15−21.
(20) Mittal, A. K.; Chisti, Y.; Banerjee, U. C. Synthesis of metallic nanoparticles using plant extracts. *Biotechnol. Adv.* **2013**, *31* (2), 346−356.
(21) Iravani, S. Green synthesis of metal nanoparticles using plants. *Green Chem.* **2014**, *13* (10), 2638−2650.
(22) Chomicki, G.; Renner, S. S. Watermelon origin solved with molecular phylogenetics including L innaean material: another example of museomics. *New Phytol.* **2015**, *205* (2), 526−532.
(23) Erhirhie, E. O.; Ekene, N. E. Medicinal values on *Citrullus lanatus* (watermelon): pharmacological review. *Int. J. Res. Pharm. Biomed. Sci.* **2013**, *4*, 1305−1312.
(24) Łopusiewicz, Ł.; Drozłowska, E.; Trocer, P.; Kostek, M.; Śliwiński, M.; Henriques, M. H.; Bartkowiak, A.; Sobolewski, P. Whey protein concentrate/isolate biofunctional films modified with melanin from watermelon (*Citrullus lanatus*) seeds. *Materials.* **2020**, *13* (17), 3876.
(25) Vinhas, A. S.; Silva, C. S.; Matos, C.; Moutinho, C.; Ferreira da Vinha, A. Valorization of watermelon fruit (*Citrullus lanatus*) byproducts: phytochemical and biofunctional properties with emphasis on recent trends and advances. *World J. Adv. Healthc. Res.* **2021**, *5* (1), 302−309.
(26) Njoya, H. K.; Erifeta, G. O.; Okwuonu, C. U.; Ezinne, E. Z. Estimation of some phytoconstituents in the aqueous extract of the endocarp, seeds and exocarp of watermelon (*Citrullus lanatus*) fruit. *J. Pharmacogn. Phytochem.* **2019**, *8* (3), 4750−4757.
(27) Taiwo, A. A.; Agbotoba, M. O.; Oyedepo, J. A.; Shobo, O. A.; Oluwadare, I.; Olawunmi, M. O. Effects of drying methods on properties of watermelon (*Citrullus lanatus*) seed oil. *Afr. J. Food. Agric. Nutr. Dev.* **2008**, *8*, 493−501.
(28) Charoensiri, R.; Kongkachuichai, R.; Suknicom, S.; Sungpuag, P. Beta carotene, lycopene, and alpha-tocopherol contents of selected Thai fruits. *Food. Chem.* **2009**, *113*, 202−207.
(29) Igwe, O. U.; Onuoha, P. U. Potentials of *Citrullus lanatus* seeds as antioxidant and antimicrobial agents and a probe of their phytochemicals. *IJCMER.* **2016**, *3* (3), 62−67.
(30) Zamuz, S.; Munekata, P. E.; Gullón, B.; Rocchetti, G.; Montesano, D.; Lorenzo, J. M. *Citrullus lanatus* as source of bioactive components: An up-to-date review. *Trends Food Sci. Technol.* **2021**, *111*, 208−222.
(31) Rizvi, S. A.; Kashanian, S.; Alavi, M. Demothoxycurcumin as a curcumin analogue with anticancer, antimicrobial, anti-inflammatory, and neuroprotective activities: Micro and nanosystems. *Nano. Micro. Biosystems.* **2023**, *2* (4), 7−14.
(32) Aderiye, B. I.; David, O. M.; Fagbohun, E. D.; Faleye, J.; Olajide, O. M. Immunomodulatory and phytomedicinal properties of watermelon juice and pulp (*Citrullus lanatus* Linn): A review. *GSC. Biol. Pharm. Sci.* **2020**, *11*, 153−165.
(33) Rashid, F.; Ahmed, Z.; Ameer, K.; Amir, R. M.; Khattak, M. Optimization of polysaccharides-based nanoemulsion using response surface methodology and application to improve postharvest storage of apple (*Malus domestica*). *J. Food. Measur. Charac.* **2020**, *14*, 2676−2688.
(34) Biswas, R.; Ghosal, S.; Chattopadhyay, A.; Datta, S. A comprehensive review on watermelon seed oil: An underutilized product. *IOSR. J. Pharm.* **2017**, *7*, 1−7.
(35) Kiani, B. H.; Haq, I. U.; Alhodaib, A.; Basheer, S.; Fatima, H.; Naz, I.; Ur-Rehman, T. Comparative evaluation of biomedical applications of zinc nanoparticles synthesized by using *Withania somnifera* Plant Extracts. *Plants.* **2022**, *11* (12), 1525−1532.
(36) Alshehri, O. M.; Alshamrani, S.; Mahnashi, M. H.; Alshahrani, M. M.; Khan, J. A.; Shah, M.; Alshehri, M. A.; Zafar, R.; Zahoor, M.; Jan, M. S.; Sadiq, A. Phytochemical analysis, total phenolic, flavonoid contents, and anticancer evaluations of solvent extracts and saponins of H. digitata. *BioMed. Res. Int.* **2022**, *2022*, 1−9.
(37) PA, W. Clinical and Laboratory Standards Institute: Performance standards for antimicrobial susceptibility testing: 20th informational supplement. *CLSI document M100-S20*. 2010. https://cir.nii.ac.jp/crid/1572261550694185984.
(38) Abdelbaky, A. S.; Abd El-Mageed, T. A.; Babalghith, A. O.; Selim, S.; Mohamed, A. M. Green synthesis and characterization of ZnO nanoparticles using *Pelargonium odoratissimum* (L.) aqueous leaf extract and their antioxidant, antibacterial and anti-inflammatory activities. *Antioxidants* **2022**, *11* (8), 1444.
(39) Xu, L.; Wang, Y. Y.; Huang, J.; Chen, C. Y.; Wang, Z. X.; Xie, H. Silver nanoparticles: Synthesis, medical applications and biosafety. *Theranostics.* **2020**, *10* (20), 8996.
(40) Siddiqi, K. S.; Husen, A. Green synthesis, characterization, and uses of palladium/platinum nanoparticles. *Nanoscale Res. Lett.* **2016**, *11*, 1−3.
(41) Nwankwo, I. U.; Onwuakor, C. E.; Nwosu, V. C. Phytochemical analysis and antibacterial activities of *Citrullus lanatus* seed against some pathogenic microorganisms. *Glob. J. Med. Res.* **2014**, *14* (4), 0975−5888.
(42) Patra, J. K.; Baek, K. H. Novel green synthesis of gold nanoparticles using *Citrullus lanatus* rind and investigation of proteasome inhibitory activity, antibacterial, and antioxidant potential. *Int. J. Nanomedicine.* **2015**, 7253−7264.
(43) Harith, S. S.; Mazlun, M. H.; Mydin, M. M.; Nawi, L.; Saat, R. Studies of phytochemical Constituents and Antimicrobial Properties of *Citrullus lanatus* Peels. *Malays. J. Anal. Sci.* **2018**, *22* (1), 151−156.
(44) Husain, F. M.; Qais, F. A.; Ahmad, I.; Hakeem, M. J.; Baig, M. H.; Masood, K. J.; Al-Shabib, N. A. Biosynthesized zinc oxide nanoparticles disrupt established biofilms of pathogenic bacteria. *Appl. Sci.* **2022**, *12* (2), 710.

https://doi.org/10.1021/acsomega.4c01554
ACS Omega 2024, 9, 16832−16841

(45) Ifeanyichukwu, U. L.; Fayemi, O. E.; Ateba, C. N. Green synthesis of zinc oxide nanoparticles from pomegranate (*Punica granatum*) extracts and characterization of their antibacterial activity. *Molecules.* **2020**, *25* (19), 4521.
(46) Umar, H.; Kavaz, D.; Rizaner, N. Biosynthesis of zinc oxide nanoparticles using *Albizia lebbeck* stem bark, and evaluation of its antimicrobial, antioxidant, and cytotoxic activities on human breast cancer cell lines. *Int. J. Nanomedicine.* **2019**, 87−100.
(47) Muhammad, W.; Ullah, N.; Haroon, M.; Abbasi, B. H. Optical, morphological and biological analysis of zinc oxide nanoparticles (ZnO-NPs) using *Papaver somniferum* L. *RSC Adv.* **2019**, *9* (51), 29541−29548.
(48) Akhter, S. M.; Mahmood, Z.; Ahmad, S.; Mohammad, F. Plant-mediated green synthesis of zinc oxide nanoparticles using *Swertia chirayita* leaf extract, characterization and its antibacterial efficacy against some common pathogenic bacteria. *Bionanoscience.* **2018**, *8*, 811−817.
(49) El-Belely, E. F.; Farag, M. M.; Said, H. A.; Amin, A. S.; Azab, E.; Gobouri, A. A.; Fouda, A. Green synthesis of zinc oxide nanoparticles (ZnO-NPs) using *Arthrospira platensis* (Class: Cyanophyceae) and evaluation of their biomedical activities. *Nanomaterials.* **2021**, *11* (1), 95.
(50) Chaudhuri, S. K.; Malodia, L. Biosynthesis of zinc oxide nanoparticles using leaf extract of *Calotropis gigantea*: characterization and its evaluation on tree seedling growth in nursery stage. *Appl. Nanosci.* **2017**, *7* (8), 501−512.
(51) Azizi, S.; Namvar, F.; Mahdavi, M.; Ahmad, M. B.; Mohamad, R. Biosynthesis of Silver Nanoparticles Using Brown Marine Macroalga, *Sargassum Muticum* Aqueous Extract. *Materials* **2013**, *6*, 5942−5950.
(52) Mendes, C. R.; Dilarri, G.; Forsan, C. F.; Sapata, V. D.; Lopes, P. R.; de Moraes, P. B.; Montagnolli, R. N.; Ferreira, H.; Bidoia, E. D. Antibacterial action and target mechanisms of zinc oxide nanoparticles against bacterial pathogens. *Sci. Rep.* **2022**, *12* (1), 2658.
(53) Meydan, I.; Burhan, H.; Gür, T.; Seçkin, H.; Tanhaei, B.; Sen, F. Characterization of *Rheum ribes* with ZnO nanoparticle and its antidiabetic, antibacterial, DNA damage prevention and lipid peroxidation prevention activity of *in vitro*. *Environ. Res.* **2022**, *204*, No. 112363.
(54) Alavi, M.; Yarani, R. ROS and RNS modulation: the main antimicrobial, anticancer, antidiabetic, and antineurodegenerative mechanisms of metal or metal oxide nanoparticles. *Nano. Micro. Biosystems.* **2023**, *2* (1), 22−30.
(55) Akbar, A.; Sadiq, M. B.; Ali, I.; Muhammad, N.; Rehman, Z.; Khan, M. N.; Muhammad, J.; Khan, S. A.; Rehman, F. U.; Anal, A. K. Synthesis and antimicrobial activity of zinc oxide nanoparticles against foodborne pathogens *Salmonella typhimurium* and *Staphylococcus aureus*. *Biocatal. Agric. Biotechnol.* **2019**, *17*, 36−42.
(56) Alghamdi, R. A.; Al-Zahrani, M. H.; Altarjami, L. R.; Al Abdulmonem, W.; Samir, N.; Said, A.; Shami, A. A.; Mohamed, W. S.; Ezzeldien, M. Biogenic Zinc oxide nanoparticles from Celosia argentea: toward improved antioxidant, antibacterial, and anticancer activities. *Front. Bioeng. Biotechnol.* **2023**, *11*, 1283898.
(57) Hayat, S.; Ashraf, A.; Zubair, M.; Aslam, B.; Siddique, M. H.; Khurshid, M.; Saqalein, M.; Khan, A. M.; Almatroudi, A.; Naeem, Z.; Muzammil, S. Biofabrication of ZnO nanoparticles using Acacia antioxidant potential against foodborne pathogens. *PLoS ONE* **2022**, *17* (1), No. e0259190.
(58) El-kady, A. M.; Hassan, S. A.; Mohamed, K.; Alfaifi, M. S.; Elshazly, H.; Alamri, Z. Z.; Wakid, M. H.; Gattan, H. S.; Altwaim, S. A.; Al-Megrin, W. A. I.; Younis, S. Zinc oxide nanoparticles produced by Zingiber officinale ameliorates acute toxoplasmosis-induced pathological and biochemical alterations and reduced parasite burden in mice model. *PLoS. Negl. Trop. Dis.* **2023**, *17* (7), No. e0011447.
(59) Chaudhary, A.; Kumar, N.; Kumar, R.; Salar, R. K. Antimicrobial activity of zinc oxide nanoparticles synthesized from Aloe vera peel extract. *SN Appl. Sci.* **2019**, *1*, 1−9.
(60) Salem, W.; Leitner, D. R.; Zingl, F. G.; Schratter, G.; Prassl, R.; Goessler, W.; Reidl, J.; Schild, S. Antibacterial activity of silver and zinc nanoparticles against Vibrio cholerae and enterotoxic *Escherichia coli*. *Int. J. Med. Microbiol.* **2015**, *305* (1), 85−95.

https://doi.org/10.1021/acsomega.4c01554
ACS Omega 2024, 9, 16832−16841